# ECHO ENABLED HIGH MODE GENERATION FOR X-RAY FELS

E. Hemsing*, SLAC National Accelerator Laboratory, Menlo Park, CA, USA
A. Marinelli, Particle Beam Physics Lab, UCLA, USA

*Abstract*

We describe a simple technique based on a modified echo-enabled harmonic generation (EEHG) scheme to manipulate the three-dimensional electron beam microbunching distribution in order to generate higher-order optical modes in an FEL. As with EEHG, the concept uses two modulators and two chicanes to produce microbunching. However, in one of the modulators, the resonant interaction with the laser has a well-defined transverse structure that becomes strongly correlated to the longitudinal microbunching distribution. Both high-harmonic frequencies and high transverse mode numbers can be generated through a transversely-dependent echo effect.

## INTRODUCTION

Modern x-ray free-electron lasers (FELs) have become a remarkable tool for probing matter at Ångstrom length and femtosecond time scales. In most X-ray FELs, the amplification process starts from noise in the electron beam (e-beam) emission spectrum, which leads to limited temporal coherence. To achieve fully coherent radiation, the echo-enabled harmonic generation (EEHG) scheme has been proposed to frequency up-convert long wavelengths with high efficiency [1, 2, 3].

The standard EEHG scheme uses two modulators and two chicanes to generate longitudinal microbunching in the e-beam at the frequency $k = nk_1 + mk_2$, where $k_1$ and $k_2$ are the frequencies of the lasers in the modulating sections. High harmonics can be obtained for large values of $n$ or $m$ by precise tuning of the modulation amplitudes and dispersions. Because the light emitted by the bunched beam will have a phase structure determined by the microbunching distribution, the transverse phase and intensity profile of the modulating lasers are typically assumed constant over e-beam profile so that the final harmonic microbunching structure has no transverse spatial dependence. This ensures maximal harmonic bunching and also facilitates emission into the Gaussian-like fundamental FEL mode, which is peaked on-axis and has an axisymmetric transverse phase profile.

There are, however, numerous theoretical and experimental contexts in which higher-order light beams are desirable or required. Of particular recent interest are *optical vortices*, or light beams that carry well-defined, discrete azimuthal phase $l\phi$ about the axis of propagation, where $l$ is an integer called the topological charge. Starting from the work of Allen [4], who showed that certain types of optical vortex modes carry discrete values $l\hbar$ of orbital angular momentum (OAM) per photon, there has been considerable work exploring the interaction of optical vortices with matter. OAM can be transferred to trapped particles [5], atoms [6], or Bose-Einstein condensates [7]. Optical vortices also have a corresponding ringlike intensity profile that can facilitate subwavelength microscopy[8], sub-diffraction fluorescence microscopy [9], imaging [10], and optical pump schemes [11]. At x-rays, optical vortices have been proposed as a method to separate quadrupolar from dipolar electronic transitions at K-edges [12].

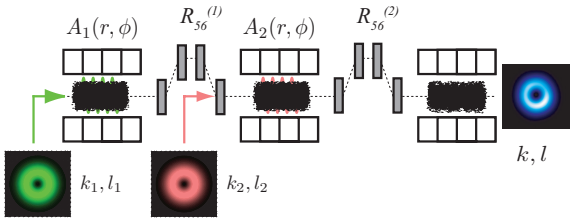


Figure 1: General setup for echo-enabled harmonic mode generation.

The generation of low-order $l$ OAM modes in FELs has been examined previously [13, 14]. Here, we examine a new variation on the EEHG scheme that enables the generation of coherent, high-order optical vortices at x-rays by up-conversion of the frequency and/or helical mode number $l$ of a microbunched e-beam. In this scheme, the energy modulation imposed on the e-beam has a well-defined helical dependence. This would be the case if the complex laser mode field profile is an OAM mode (as in Figure 1), or, more generally, if the resonant modulator phase bucket has a helical phase structure [15]. In contrast to standard EEHG, recoherence of the imprinted helcial modulations here occurs as a correlated function of transverse position in the e-beam after passage through the beamline. As a result, both the frequency and helical mode number $l$ can be up-converted through a process we refer to as echo-enabled harmonic mode generation, or EEHMG. The final, highly-correlated helical microbunched distribution can be tailored to preferentially emit optical vortices with varying $l$ values and harmonics in a downstream radiator through proper adjustment of the laser modulation profile, amplitude, and beamline dispersion.

A striking feature of the spatial recoherence effect in EEHMG is that it allows large up-conversion of the frequency and $l$ mode either simultaneously, or independently. By upconverting both together, one can generate large $l$ modes at harmonics. Alternately, large frequency harmonics can be generated without changing the magnitude of $l$ so that the helical distribution generated at one frequency can be passed to a vastly different frequency.

* ehemsing@slac.stanford.edu

*Presented at the 3rd International Particle Accelerator Conference (IPAC 2012)*
*New Orleans, Louisiana, USA, May 20 - 25, 2012*

*Work supported in part by US Department of Energy under contract DE-AC02-76SF00515.*

## FORMULATION

The modified echo scheme is shown Figure 1. The e-beam distribution at the entrance to the first modulator is given by $f_i(r, \phi, p)$, where $r$ and $\phi$ are the radial and azimuthal coordinates, $p = (E - E_0)/\sigma_E$ is the scaled electron energy with respect to the central beam energy $E_0 = \gamma mc^2$, and $\sigma_E$ is the rms energy spread. We consider the complex modulation amplitude in the first modulator to be of the form $A_1(r, \phi) = \overline{A}_1(r)\text{Exp}(il_1\phi)$, where $l_1$ is an integer that describes the azimuthal phase variation across the profile, and $\overline{A}_1$ is the radially dependent field amplitude. At the exit of the first modulator section, the beam energy is modulated such that an electron acquires a new energy $p' = p + \overline{A}_1 \sin(k_1 z + l_1\phi)$ where $k_1 = 2\pi/\lambda_1$ is the laser frequency and $z$ is the initial longitudinal position of the electron in the beam. Due to the transverse dependence, the energy kick depends on the electron's azimuthal position $\phi$ radial position $r$. Note that the mathematical form of the modulating field is in fact quite general, in that it describes a modulation generated either by an OAM laser seed, or by the interaction of the e-beam with a Gaussian laser at harmonics of a helical undulator, as in HGHMG seeding [14]. The beam then passes through a longitudinally dispersive section characterized by the matrix element $R_{56}^{(1)}$, which shifts the electron to the position $z'$ according to $z' = z + B_1 p'/k_1$, where $B_1 = R_{56}^{(1)} k_1 \sigma_E/E_0$. The beam is then modulated by the second laser, with frequency $k_2 = 2\pi/\lambda_2$, in the second modulator according the the field distribution $A_2(r, \phi) = \overline{A}_2(r)\text{Exp}(il_2\phi)$. The new energy is $p'' = p' + \overline{A}_2 \sin(k_2 z' + l_2\phi)$. The second chicane, with dispersion $R_{56}^{(2)}$, transforms the longitudinal position as, $z'' = z' + B_2 p''/k_1$, where $B_2 = R_{56}^{(2)} k_1 \sigma_E/E_0$. In terms of the final variables at the end of the last dispersive element, the e-beam bunching factor at the frequency $k$ and at the azimuthal mode $l$ is given by

$$b^{(l)}(k) = \frac{1}{N_0} \left| \langle e^{-ikz'' - il\phi} f_f(r, \phi, z'', p'') \rangle \right| \quad (1)$$

where $f_f(r, \phi, z'', p'')$ is the final e-beam distribution, and brackets denote averaging over the final coordinates. Transforming back to the initial coordinates, the exponential term is then,

$$\begin{aligned} \text{Exp}\left[-ikz'' - il\phi\right] &= \textstyle\sum_{n,m} e^{-ikz - il\phi - i\frac{k}{k_1} p(B_1 + B_2))} \\ &\times e^{in(k_1 z + l_1\phi) + im(k_2 z + l_2\phi + KB_1 p)} \\ &\times J_n\left[\overline{A}_1(mKB_1 - \tfrac{k}{k_1}(B_1 + B_2))\right] J_m\left(-\tfrac{k\overline{A}_2 B_2}{k_1}\right) \end{aligned} \quad (2)$$

where $K = k_2/k_1$. Averaging over $z$ picks out the dominant microbunching frequencies,

$$k \equiv ak_1 = nk_1 + mk_2, \quad (3)$$

where $a = n + mK$. This is precisely the same frequency conversion relation as EEHG. Here, however, there is also an $l$-mode conversion relation, found by averaging over the azimuthal coordinate $\phi$. Assuming an axisymmetric, uncorrelated initial e-beam distribution $f_i(r, \phi, p) = N_0(2\pi)^{-1/2} e^{-p^2/2} f_0(r)$, the $\phi$ integral in (1) is straightforward, and the final azimuthal density mode excited in the beam has the same up-conversion as the frequency:

$$l = nl_1 + ml_2. \quad (4)$$

One can therefore simultaneously convert both the frequency and azimuthal mode number of the microbunched distribution in EEHMG. The final bunching factor is expressed in general as,

$$b_{n,m}^{(l)} = \left| e^{-\xi^2/2} \int J_n\left(\overline{A}_1 \xi\right) J_m\left(-a\overline{A}_2 B_2\right) f_0(r) r dr \right| \quad (5)$$

where $\xi = -(nB_1 + aB_2)$. If the transverse variation of the fields is negligible over the e-beam such that $l_1, l_2 = 0$, $\overline{A}_1 = A_1$ and $\overline{A}_2 = A_2$, this reduces to the expression in [1] for standard EEHG. With $\overline{A}_2 = B_2 = 0$, the general formula for HGHMG is recovered [14].

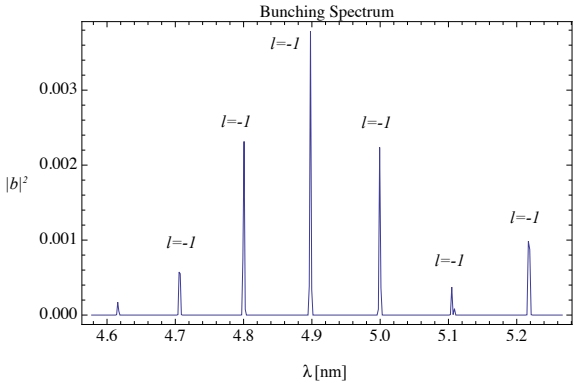


Figure 2: Bunching spectrum of $l = -1$ helical mode in $\sigma_t$=10 fs beam optimized for $n = -1$, $m = 50$ with $l_1 = 1$, $l_2 = 0$, $A_1 = A_2 = 3$, $B_1 = 16.94$, $B_2 = 0.36$, $\lambda_1 = \lambda_2 = 240$ nm

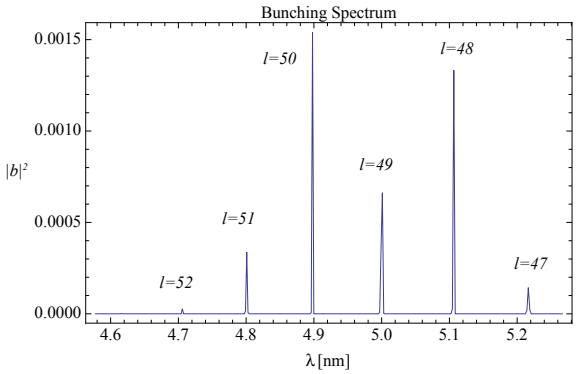


Figure 3: Bunching spectrum optimized for $n = -1$, $m = 50$. Both the OAM mode and frequency are up-converted with $l_1 = 0, l_2 = 1, A_1 = A_2 = 3, B_1 = 29.5, B_2 = 0.61$, $\lambda_1 = \lambda_2 = 240$ nm

## EXAMPLES

Among the numerous possible combinations of helical mode numbers $l_1$ and $l_2$ and harmonic numbers $n$ and $m$, two examples illustrate the primary aspects. First consider an $l_1 = 1$ modulation in the first stage of Fig 1 from a field of the form $\overline{A}_1(r) = A_1(\sqrt{2}r/w_0)^{|l_1|}e^{-r^2/w_0^2}$, where $w_0$ is the laser spot size. The e-beam is then modulated in the second stage by a simple Gaussian laser with $l_2 = 0$. From Eq. (4) the final azimuthal mode number is given by $l = nl_1$, and thus does not depend on the potentially large harmonic number $m$ of the frequency up-conversion. As with EEHG, for $m \gg 1$, the bunching factor is maximized when $n = -1$ and $B_1, B_2$ have the same sign. Thus, the final mode number is $l = nl_1 = -1$. Figure 2 shows the microbunching bunching spectrum (calculated from Eqs. 1 and 2 for a finite beam with rms length $c\sigma_t$) from a helical modulation in the first stage. The spectrum is composed of different frequency spikes, each of which corresponds to an $l = -1$ helical modulation. In a radiator, this beam will emit light with a helical phase at the frequency (or frequencies) within the radiator bandwidth.

It is interesting to note that the final mode $l$ has the opposite sign as $l_1$ by virtue of the choice $n = -1$. This ability to transform between different azimuthal mode numbers is a key feature of the 3D echo recoherence effect. Consider a reversal of the previous arrangement, where now, the helical modulation is performed in the second modulator. The first modulation has no transverse dependence ($l_1 = 0$), so that the final azimuthal mode number is then $l = ml_2$, which can be made large during harmonic upconversion for $m \gg 1$. The spectrum shown in Figure 3 displays the result from this arrangement where each frequency peak is now characterized by a distinct $l$ value. Thus, a narrowband radiator can be tuned to pick out a single peak to emit a coherent vortex with a specific value of topological charge. Large $l$ modes are not amplified in FELs due to their large emission angles and weak coupling, but can be emitted superradiantly in an undulator or from a CTR foil.

It is noted that, not only does the long term memory of the correlated phase space have to be preserved to obtain the high-harmonic values, but the highly correlated *helical* structure is also highly susceptible to wash out from transverse motion of the electrons. Optimization of this scheme requires precise tuning of the betatron phase advance (which should be a multiple of $\pi$ ) in order to reestablish the 3D structure. Note that odd-$\pi$ phase angles mirror the $x$ and $y$ electron positions across the $z$ axis and thus change the sign of odd $l$ modes (even modes are unchanged).

## ACKNOWLEDGMENTS

Work supported by U.S. DOE under Contract Nos. DE-AC02-76SF00515 and DE-FG02-07ER46272.

## REFERENCES

[1] G. Stupakov. Using the beam-echo effect for generation of short-wavelength radiation. Phys. Rev. Lett., 102:074801, Feb 2009.

[2] Dao Xiang and Gennady Stupakov. Echo-enabled harmonic generation free electron laser. Phys. Rev. ST Accel. Beams, 12:030702, Mar 2009.

[3] D. Xiang, E. Colby, M. Dunning, S. Gilevich, C. Hast, K. Jobe, D. McCormick, J. Nelson, T. O. Raubenheimer, K. Soong, G. Stupakov, Z. Szalata, D. Walz, S. Weathersby, and M. Woodley. Evidence of high harmonics from echo-enabled harmonic generation for seeding x-ray free electron lasers. Phys. Rev. Lett., 108:024802, Jan 2012.

[4] L. Allen, M. W. Beijersbergen, R. J. C. Spreeuw, and J. P. Woerdman. Orbital angular momentum of light and the transformation of laguerre-gaussian laser modes. Phys. Rev. A, 45(11):8185–8189, Jun 1992.

[5] M. E. J. Friese, J. Enger, H. Rubinsztein-Dunlop, and N. R. Heckenberg. Optical angular-momentum transfer to trapped absorbing particles. Phys. Rev. A, 54(2):1593–1596, Aug 1996.

[6] A. R. Carter, M. Babiker, M. Al-Amri, and D. L. Andrews. Generation of microscale current loops, atom rings, and cubic clusters using twisted optical molasses. Phys. Rev. A, 73:021401, Feb 2006.

[7] M. F. Andersen, C. Ryu, Pierre Cladé, Vasant Natarajan, A. Vaziri, K. Helmerson, and W. D. Phillips. Quantized rotation of atoms from photons with orbital angular momentum. Phys. Rev. Lett., 97:170406, Oct 2006.

[8] Alexander Jesacher, Severin Fürhapter, Stefan Bernet, and Monika Ritsch-Marte. Shadow effects in spiral phase contrast microscopy. Phys. Rev. Lett., 94:233902, Jun 2005.

[9] P. Török and P. Munro. The use of gauss-laguerre vector beams in sted microscopy. Opt. Express, 12(15):3605–3617, 2004.

[10] B. Jack et al. Holographic ghost imaging and the violation of a bell inequality. Phys. Rev. Lett., 103(8):083602, Aug 2009.

[11] J. W. R. Tabosa and D. V. Petrov. Optical pumping of orbital angular momentum of light in cold cesium atoms. Phys. Rev. Lett., 83(24):4967–4970, Dec 1999.

[12] Michel van Veenendaal and Ian McNulty. Prediction of strong dichroism induced by x rays carrying orbital momentum. Phys. Rev. Lett., 98(15):157401, Apr 2007.

[13] Shigemi Sasaki and Ian McNulty. Proposal for generating brilliant x-ray beams carrying orbital angular momentum. Phys. Rev. Lett., 100(12):124801, 2008.

[14] E. Hemsing, A. Marinelli, and J. B. Rosenzweig. Generating optical orbital angular momentum in a high-gain free-electron laser at the first harmonic. Phys. Rev. Lett., 106(16):164803, Apr 2011.

[15] E. Hemsing, P. Musumeci, S. Reiche, R. Tikhoplav, A. Marinelli, J. B. Rosenzweig, and A. Gover. Helical electron-beam microbunching by harmonic coupling in a helical undulator. Physical Review Letters, 102(17):174801, 2009.